ASPRS Annual Conference, Denver, CO, May 23-28, 2004

TRIANGULATION BASED HIERARCHICAL IMAGE MATCHING FOR MARS DEM GENERATION USING MOC NA STEREO IMAGES

Rajagopalan Rengarajan **Jong-suk Yoon** **Jie Shan**

Geomatics Engineering
School of Civil Engineering
Purdue University
550 Stadium Mall Dr.
West Lafayette, IN 47907-2051

ABSTRACT

Traditional image matching approaches often fail in processing Mars Global Surveyor stereo images because of low contrast and insufficient number of features. Reliable and precision matching tool is needed for precise Mars digital elevation model generation. This paper presents a hierarchical image matching approach. First, a number of well identified points are manually measured in a stereo pair. These measurements are input into a commercial digital photogrammetric tool as 'seed points' to generate more corresponding points. After that, the Delaunay triangulation network is formed for those seed points. The initial correspondence of an interest point on the other image is located by using the bilinear polynomial transformation whose coefficients are determined by six points closest to the interest point in the triangle. The conjugate point of the interest point in each triangle of the network is determined by using the parameters of the polynomial equation. In the next iteration, all the above generated corresponding points and the original seed points will be triangulated and the network will be densified in the same manner. This process repeats until the required point density is achieved. This initial prediction is then refined by using cross correlation and the least squares matching approaches. Based on this approach, we have matched stereo image pairs over selected landing sites for the Mars Exploration Rover mission. Assessment of image results suggests a matching consistency of better than one pixel. Presented in this paper are results of detailed matching quality evaluation and the generated digital elevation models.

INTRODUCTION

Digital elevation model (DEM) provides the surface topography for various applications of engineering and science. This paper purposes to generate DEM of Mars for investigation Martian topography. Various approaches are actively proposed to generate topography products on Mars recently. Ivanov and Lorre (2002) generated topography using correlation matching method from stereo pairs of low-resolution image from Mars Global Surveyor (MOC) Wide Angle (WA). Krik at al. (2002) reported the generation of DEM from MOC NA images controlled by laser altimetry data. In this paper, image matching technique and photogrammetric principle are used to generate the DEM of Mars from high-resolution stereo images of MGS Narrow Angle (NA). Because the resolution of MOC NA images are 4 or 5 meter per pixel the DEM generated from this study will be high-resolution, 10 meter DEM.

DEM generation for Mars provides more challenges than the conventional DEM generation over Earth. The primary reason is due to the lack of control and secondly, the images obtained from Mars do not have sufficient contrast as that of Earth imagery. As a result of this, the conventional tools do not always provide the enormous number of conjugate points required to create DEM. An image matching approach that we proposes in this paper recursively refines the matching results by improving the approximations obtained at each level.

The study sites for this paper are three sites among the landing candidate sites for MER: EOS chasma, Gusev crater and Isidis Planitia. There are two main steps involved in generation of DEM. The first is matching algorithm to determine the correspondence points in the left and right stereo pair, while the second involves the use of the corresponding points to create the DEM by using photogrammetric and interpolation method. These two main steps are explained individually in this paper.

IMAGE MATCHING METHOD

Image matching algorithm proposed here matches the stereo images so that the matched images can be used to create DEM. The result of matching, and the density of the points greatly affects the quality and the accuracy of DEM. As conventional algorithms of matching do not always provide more number of these conjugate point pairs, it is necessary to develop a method which could identify more conjugate pairs in the image with improved accuracy and reliability.

The images from MGS have different characteristics from common satellite images over earth. MGS MOC imagery in general has very low contrast and there are not many features on Martian surface except several craters and rocks. Those properties are main obstacles for applying traditional matching algorithms to generate DEM on Mars. Considering uniqueness of MOC image and Martian surface, hierarchical matching approach is proposed to meet with reliable and precise matching result. The main idea of hierarchical matching algorithm is improvement of matching results in every step by reducing the error obtained in the previous step.

The image matching methodology discussed in this paper can be summarized by three steps in general. In the first step, the two images are matched approximately by fitting a polynomial equation. The section of an image represented by a triangle is fitted with a unique set of polynomial transformation. Thus each triangle/different sections of image is represented by different set of parameters. These different set of parameters fit the two images much better than single polynomial equation of higher order for the whole image. Hence, this technique improves the overall prediction of conjugate points. The triangulation is done recursively to increase the density of points. The second step of matching is a refinement based on cross-correlation. The results obtained in the first step are used as approximations to refine using cross-correlation. In the last step, the refined coordinates from the cross-correlation technique are finally used as input to accurately predict the conjugate points by least square matching technique. Figure 1 describes three main steps and other associated procedures for image matching algorithm. Following the procedures in Figure 1, comprehensive explanation about each procedure is presented in the following part of image matching methodology.

Seed points and Delaunay triangulation

First, about two dozens of well defined points are manually measured in a stereo pair. The manually collected points are evenly distributed over the corresponding area on stereo pairs. These measurements are given as input to commercial digital photogrammetric tool as seed points to generate more conjugate points. However, our experience shows the capabilities of this automatic process is very limited. For example, for Gusev crater region, we could only generate 162 such conjugate points. Table 1 shows the number of conjugate points of all study sites.

Apparently, this amount is not sufficient to generate the DEM for the entire stereo model. The fine DEM of the region can be generated with better accuracy if and only if we have more number of corresponding or conjugate points. Hence the results obtained from the commercial tool can be used as the input for triangulation network of our image matching algorithm.

The points obtained from the above method are used to fit a “Delaunay” triangulation network. The Delaunay triangulation maximizes the minimum angle for all triangular elements which is the requirement for good quality finite elements. Hence the triangulation network obtained would be the less ill conditioned triangles compared with other triangulation network algorithms. Once the triangulated mesh is created, the next step involves the selection of a point inside each triangle.

Selection of interest points

Inside each triangle a unique point is selected. This point is selected based on the geometric characteristics of the triangle. It is required that the conjugate point pairs are more uniformly distributed over the entire image to get more accurate DEM for the overlapped region of the image. Thus, to obtain uniform point density over the overlapped region, we have selected the centre of each triangle as the interest point. This is the point which is equi-distant from three vertices of the Delaunay triangle.

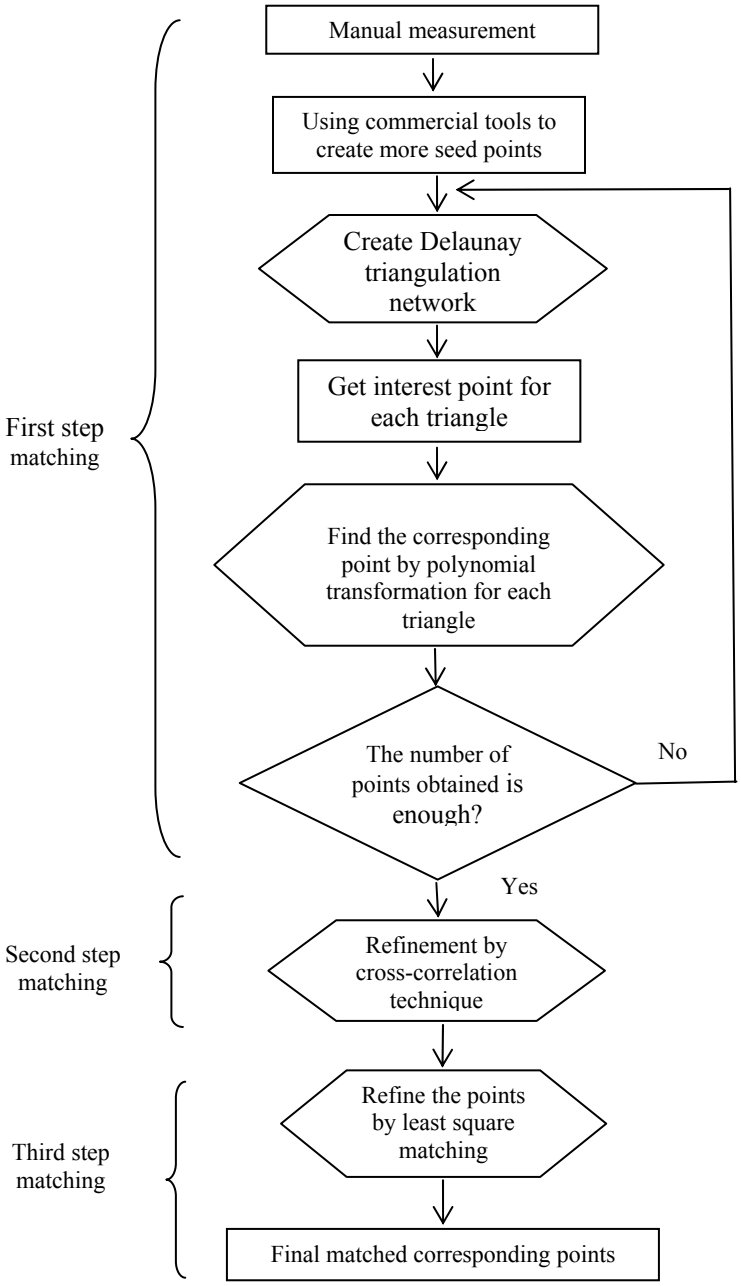

Figure 1. Flowchart of matching algorithm showing three main steps and comprehensive procedure

However, our current work is more oriented towards using the radiometric information of the image along with the geometric characteristics of the triangle. Instead of selecting the center of the triangle, the interest point is selected based on an objective function. The objective function uses the texture/gradient information of the image along with its distance to the center of the triangle. The gradient information helps to select those points which has higher contrast while the second criterion (distance to center) makes sure that the distribution of the seed points are not clustered only on certain regions of the images, but distributed uniformly over the entire image.

The distance value with its gradient number is used in the objective function to determine the best interest point for each of the triangle. The objective function that can be used to determine the interest point would look like the one shown below in equation 1.

$$f = w_D N_D + w_G N_G \quad (1)$$

where, $N_D = \frac{\min(dist_i)}{dist_i}$, $N_G = \frac{DN_i}{\max(DN_i)}$

W_D and W_G are the weight associated for the distance value and the gradient value respectively
N_D and N_G are the normalized distance and the normalized gradient value respectively ranging from 0 to 1
DN_i is the gradient value for a point P_i inside the triangle
$dist_i$ is the distance of the point P_i from the centroid of the triangle

The point where the objective function *f* maximizes would give the location of the interest point within a triangle. Weights can be altered at various iterations to accommodate a compromise between the distribution of points and the use of gradient points. We are currently working towards using the above approach.

Polynomial parameter estimation

After determining the interest point inside each triangle, the corresponding location of this interest point in the other image is determined by fitting the polynomial equation between the right and left images. In order to fit the eight parameter bilinear transformation, we need minimum of four point pairs. We have used the three vertices points of the triangle. Hence we need one more point other than the three vertices, as a minimum condition to fit the polynomial function. We however have used six points in total to have better redundancy. The six points are chosen such that the points are well distributed and closer to the interest point. Figure 2 illustrated the six points considered to estimate the parameters of the polynomial equation.

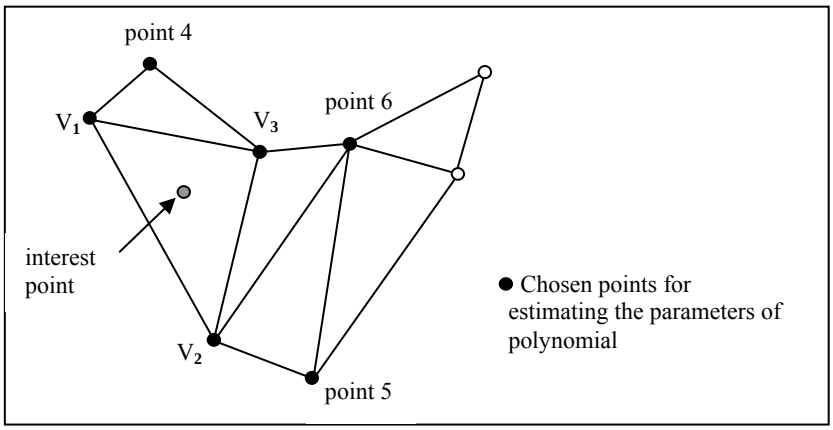

Figure 2.Triangulation and densification of seed points

Since the interest point lies inside a triangle, the three vertices of the triangle are used as three out of six points to estimate the polynomial parameters. Three other points are selected such that each of them is closer to each of the vertex. i.e., point 4 (as shown in Figure 2) is closer to the vertex v_1. Similarly, the other two points are closer to the other two vertices correspondingly. Thus a total of six closest points are obtained for the interest point inside the triangle, and these points have their coordinates known in both right and left images.

These six points are used to fit a bilinear polynomial equation between the right and left image. It is an eight parameter transformation (Equation 2) between the left and right image within the region selected by the six points. To solve this set of equations, we have used the least squares approach and the parameters are adjusted accordingly to minimize the squared error. The parameters obtained are used to predict the location of the corresponding point in the other image for the selected interest point.

$$x_R = a_0 + a_1 x_L + a_2 y_L + a_3 x_L y_L$$
$$y_R = b_0 + b_1 x_L + b_2 y_L + b_3 x_L y_L \quad (2)$$

where, $(x_R, y_R), (x_L, y_L)$ are right and left image coordinates respectively,
$a_0, a_1, a_2, a_3, b_0, b_1, b_2, b_3$ are the eight transformation parameters.

This method assumes that the variation between right and left image in the smaller region enclosed by six points vary by the bilinear polynomial function. This assumption is also true due to the consideration of small region, which doesn't exhibit dramatic changes in the terrain. That is, the terrain changes are very moderate within the region selected by the six points. At the end of this step, we can identify the corresponding points in the other image for the interest point in each triangle of master image. Thus the original set of the corresponding points are now increased by the original set of points and a point for each of the triangle formed from the triangulated network.

Now in the next iteration of the calculation, the new set of point pairs (interest points location in left and right image) are added to the original set of point pairs to obtain a new set of corresponding points between left and right image. This new set is used to form a triangulated network, and an interest point in each triangle is selected as discussed above and its corresponding point in other image is determined in a similar way. This step is continued recursively until a required number or density of corresponding points between left and right image are obtained.

Refinement by cross-correlation

From the previous step, we have enormous conjugate points required to produce dense DEM for the region. But the accuracy of the matching is not very accurate to 1 or 2 pixels as needed. Therefore, moving window on left and right images is used to determine the location of conjugate point in right image to achieve less than 1 or 2 pixel error. Then, final refined location of conjugate point is determined by cross-correlation number.

Figure 3 illustrates the target window and search window on left and right images for the cross-correlation. First, a window centered at the initial location of the left image is defined as the target window. The window size used for target image is 13 by 13 pixels. Another window is centered on the approximate location of the corresponding conjugate point in the right image which was obtained from the previous step. This window is called as search window. The window size used for search window is 17 by 17 pixels. The 13 by 13 target window is moved over the search window and each set of values are compared with the target window for estimating the correlation coefficient. The gray values in the target window and search window are used to calculate the cross-correlation value in Equation 3. The final location is at the place where the correlation coefficient reaches the maximum within the searching window.

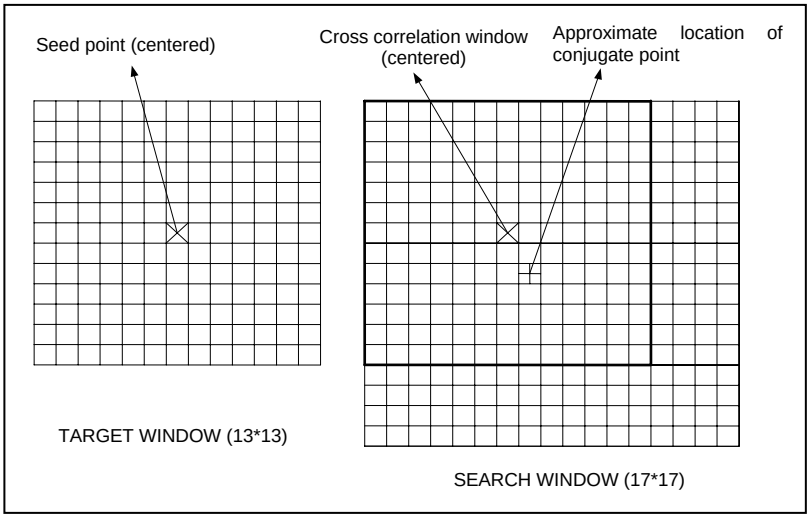

Figure 3. Target and search windows on left and right images

$$\rho = \frac{\sum_{i=1}^{n}(g_{Li} - \overline{g_L})(g_{Ri} - \overline{g_R})}{\sqrt{\sum_{i=1}^{n}(g_{Li} - \overline{g_L})^2 \sum_{i=1}^{n}(g_{Ri} - \overline{g_R})^2}} \quad (3)$$

where

$g_{Li}, \overline{g_L}$ are the intensity values of the left image at i[th] location and mean intensity for the window correspondingly

$g_{Ri}, \overline{g_R}$ are the intensity values of the right image at i-th location and mean intensity for the window correspondingly

In this process, the left image is used as a master/target image and the right image is used as a search image or a slave image. The number of conjugate points in this step remains the same as in the previous step, as we are refining the location of the conjugate point with in the search window of the right image. The next step of refinement is to accurately determine the matching points to sub-pixel level accuracy using Least Square Matching technique.

Refinement by Least Square Matching

In order to achieve sub pixel accuracy using the least squares matching, certain conditions are to be fulfilled. The initial approximations should be accurate to less than 1 to 2 pixels. If this condition is not satisfied, then the least square matching will stop and the matching results are taken as the same as the one from the cross correlation step.

The approximation used for the least square matching is obtained from the previous step where, the images are matched based on the cross-correlation. In the least square matching, pixel gray values in one image are arbitrarily chosen to be the observables, while pixel gray values in the other image are chosen to be constants. In our case, we have chosen the left image grey values as constants, while the pixel grey values of right images as observables.

The simplified equation considering the radiometric and geometric parameters would be Equation 4 in which the two coordinate systems are related by the six parameter transformation as Equation 5.

$$g(x_L, y_L) = k_1 h(x_R, y_R) + k_2 \quad (4)$$

$$x_R = a_1 x_L + a_2 y_L + a_3$$
$$y_R = b_1 x_L + b_2 y_L + b_3 \quad (5)$$

where, xL and yL: image coordinates of the left image xR and yR: image coordinates of the right image

$a_1, a_2, a_3, b_1, b_2, b_3, k_1, k_2$: Parameters

Since the images are nearly aligned and are radiometrically similar, we can take the initial approximation parameter vector to be,

$$[a_1, a_2, a_3, b_1, b_2, b_3, k_1, k_2] = [1, 0, 0, 0, 1, 0, 1, 0]$$

The least square adjustment by indirect observation is used to solve the equation and to determine the adjusted values. In this approach a window size of 11 by 11 pixels is considered for matching the region between right and left image. The adjusted values are the final result of the matching process which matches the images to less than 1 pixel accuracy at the corresponding points.

Image matching quality assessment

After applying matching algorithms, the number of corresponding points sufficiently increases to generate DEM for three study site. In the first step in Figure 1, seed points are searched manually and automatically in commercial program. Table 1 shows the number of seed points in the beginning of matching algorithm. In addition, the final number of matched points after applying proposed matching algorithm is also presented in Table 1.

Table 1. Number of seed points and corresponding points after image matching

	EOS crater	Gusev crater	Isidis
# of Seed point	162	162	55
# of matching point	25,110	38,276	24,300

Figure 4 illustrated the increase of the number of matching points after iteration. The upper row of Figure 4 is overlaid matching points with the left image while the bottom row is overlaid matching points with the right image, both for the Gusev crater. From the left side, each row shows the image of seed points which are matched from the commercial program, matching points after second iteration, fourth iteration and last iteration. The number of matching points is remarkably increased.

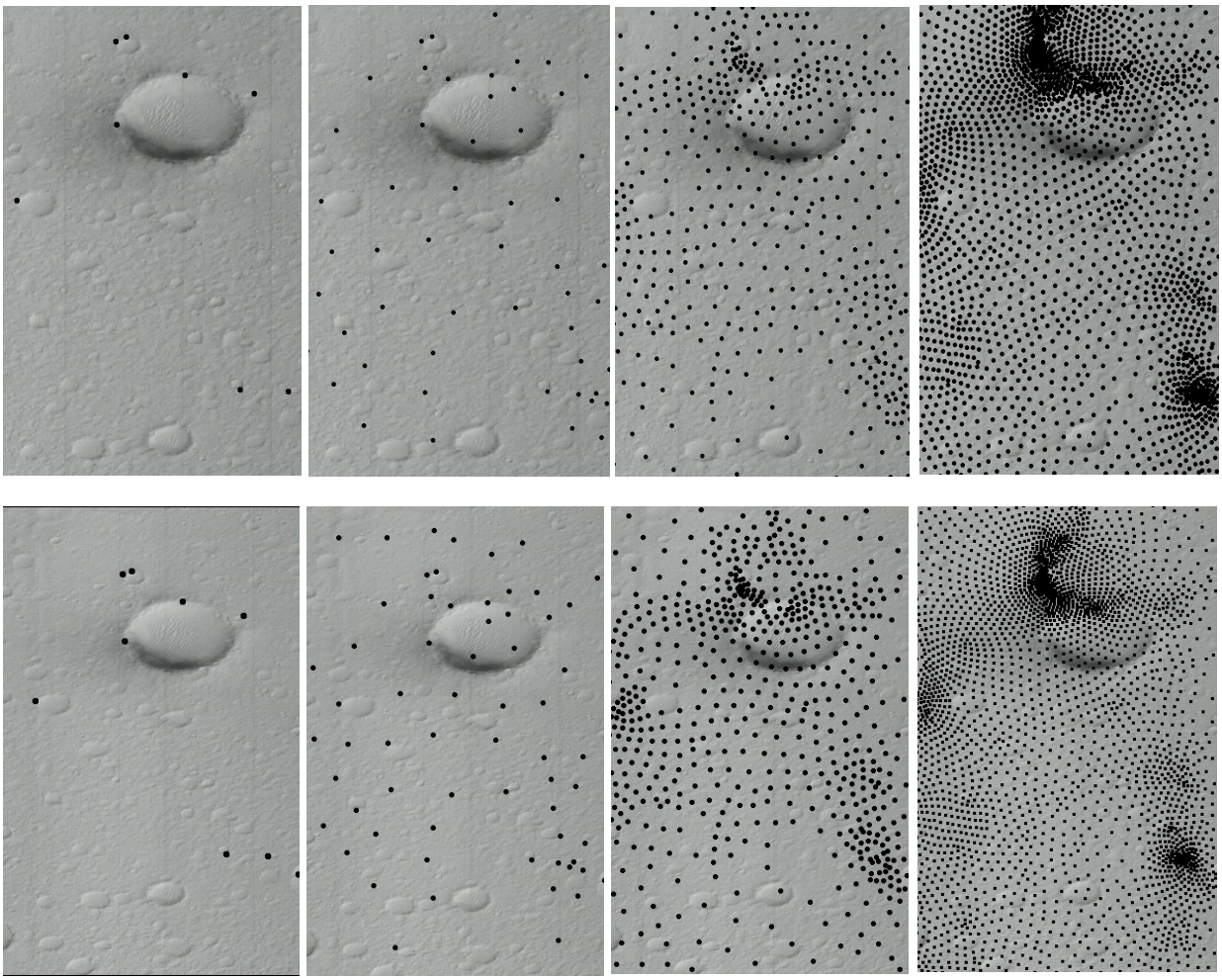

Figure 5. Number of matching points in iteration (upper images: left image; bottom images: right images; from left to right: **seed point, 2nd, 4th, and last iteration; Gusev Crater site)**

Figure 5 shows the matching point's precision by visually comparing left and right images of Gusev crater. Circles on Figure 5 indicate some matched feature points.

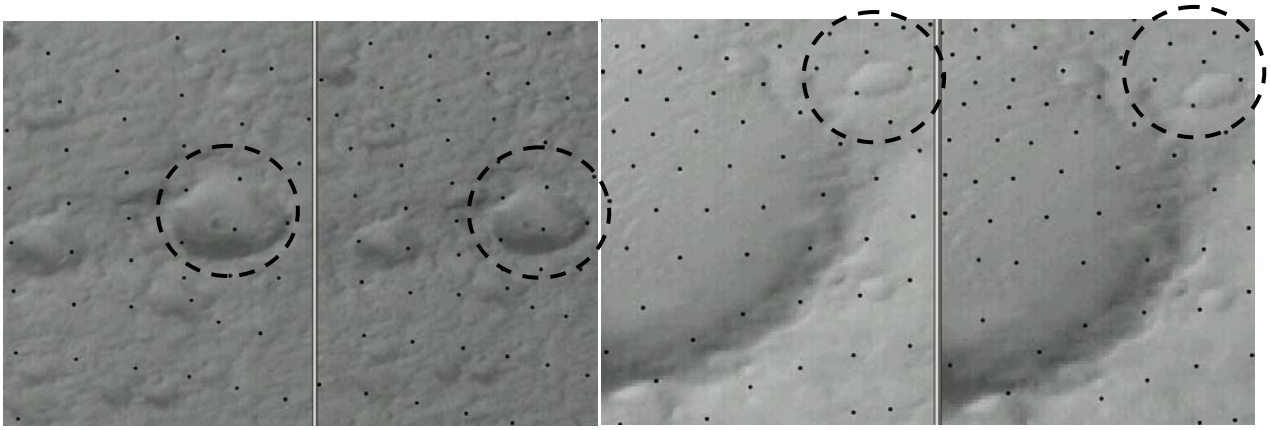

Figure 6. Image matching results of Gusev crater site (Left two: upper part of the image; Right two: bottom part of the image)

The final step in this level of matching process is to assess the quality of this process. As an internal check, we exchange the roles of the left and the right images. Now, the right image acts as the master image, and the left image as the slave image. The window size for the target and search window remains the same as in the previous case. The conjugate point obtained for the right image is now used as the target point whose corresponding location is found on the left image. The difference between the original location of the point on the left image and its determined location by reversing is found and is also shown graphically below in Figure 6.

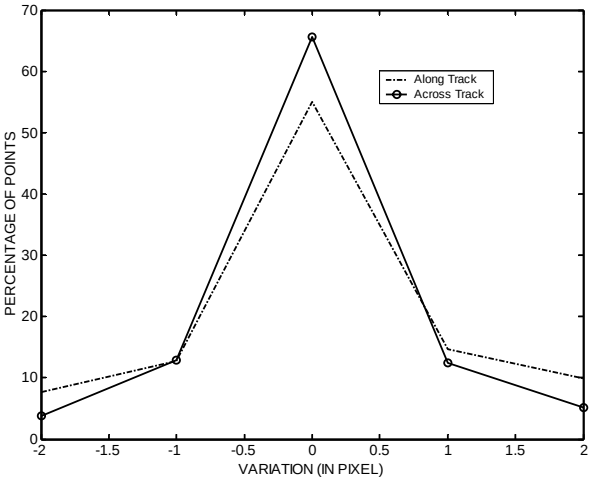

Figure 6. Difference in pixels in across and along track (forward and reverse)

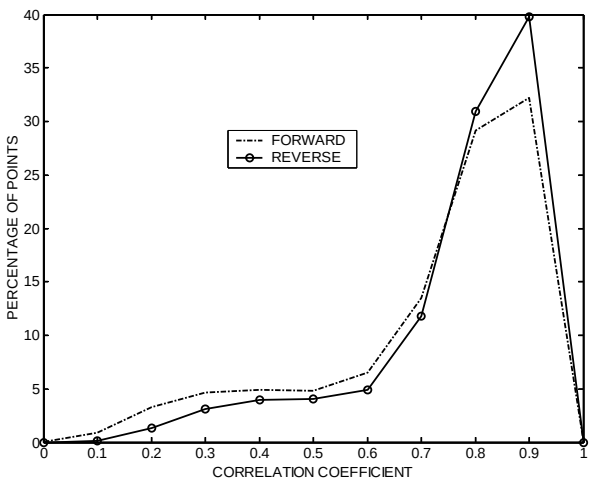

Figure 7. Correlation coefficient values while running the the algorithm in forward and reverse directions

The mean is 0.06 pixels and 0.02 pixels in the along tack and across track respectively. The standard deviation is 0.98 pixels and 0.78 pixels in the along tack and across track respectively. The figure 6 clearly shows that about 65% of the points are determined to their same location by reversing the algorithm. It is also clearly seen that more than 90% of the points lie within less than 1 pixel difference and all the points lie with in 2 pixel difference while running the algorithm by exchanging the right and left images. The mean is zero while the standard deviation for all the matched points is less than 1 pixel. This shows the high consistency of the process.

Figure 7 shows the correlation coefficient values obtained by running the algorithm by exchanging the right and left images. The graph shows that about 85% of points were determined with higher correlation coefficient (>0.7) which signifies more probable correspondence between the right and left conjugate point detection. Further, the

pattern of the curve remains the same irrespective of using the right image as master image or the left image as master image.

The above results indicate the uncertainty of the matching process, and from the figure 6 and figure 7 we can conclude that the algorithm works reliably and effectively in detecting the conjugate points. The quality assessment of the matching results clearly shows that the matching algorithm is accurate enough to be used as an input to generate the DEM.

DEM GENERATION

As the second main step in DEM generation, this section will explain processes to calculate the ground coordinates of matching points and their orthometric heights, and the interpolation method to generate a regular gird DEM.

Photogrammetric procedure: Intersection

The collected corresponding points are used for the generation of a DEM through photogrammetric procedure. With the image coordinates of matching points on both MOC stereo images and the exterior orientation, X, Y and Z coordinates of matching points are calculated with the collinearity equations. Exterior orientation sets which are the position and pointing information of the camera are initially taken from SPICE (Spacecraft, Planet, Instrument, C-matrix and Event) based on the navigation data and then refined through a bundle adjustment. SPICE provided by Navigation and Ancillary Information Facility (NAIF) of NASA is a library to extract the satellite orbital information and camera geometric information. Because MOC images are linear pushbroom images, the exterior orientation is dependent on time. According to the time of an image line, the exterior orientation sets are calculated over the image for a specific time interval, and then the motion of the sensor at any line of an image are modeled by a second order polynomial.

Equation 6 explains the calculation of X, Y and Z coordinates using collinearity equations (Mikhail et al, 2001). With exterior orientation and image coordinates of matching points on stereopair images, two collinearity equations per each image for a matching point can be formed as shown in Equation 6. Due to the two stereo images used in this research, a total of four collinearity equations for a point can determine the unknown X, Y and Z coordinates.

$$\begin{bmatrix} X - Xc \\ Y - Yc \\ Z - Zc \end{bmatrix} = \begin{bmatrix} m_{11} & m_{12} & m_{13} \\ m_{21} & m_{22} & m_{23} \\ m_{31} & m_{32} & m_{33} \end{bmatrix} \begin{bmatrix} 0 \\ y \\ -f \end{bmatrix} \tag{6}$$

$$\frac{X - Xc}{Z - Zc} = \frac{m_{12}y - m_{13}f}{m_{31}y - m_{33}f} \qquad \frac{Y - Yc}{Z - Zc} = \frac{m_{22}y - m_{23}f}{m_{31}y - m_{33}f}$$

where, X,Y,Z : Cartesian coordinates, Xc,Yc,Zc: satellite position
y: across track image coordinates
f: focal length
m_{12}…m_{33}: components of rotation matrix

Coordinates and height conversion

Such calculated Cartesian coordinate need to be converted to geographic coordinates or a map projection and orthometric height for DEM production. This two step conversion process is outlined below. First, geographic coordinates are obtained from Cartesian coordinates. Equation 7 shows Conversion from Cartesian coordinates to ellipsoid longitude (λ_e), latitude (φ_e) and height (h_e).

$$\lambda_e = \arctan\left(\frac{Y}{X}\right)$$

$$\varphi_0 = \arctan\left(\frac{Z}{\sqrt{X_2 + Y_2}}\right), \quad \varphi_e = \arctan\left(\frac{Z + N_0 e^2 \sin(\varphi_0)}{\sqrt{X^2 + Y^2}}\right) \quad \text{iteration} \quad |\varphi_e - \varphi_0| < \varepsilon \tag{7}$$

$$h_e = \sqrt{X^2 + Y^2 + (Z + Ne^2 \sin^2 \varphi)} - N$$

where, $N_0 = \frac{a}{\sqrt{1 - e^2 \sin^2(\varphi_0)}}$, toleranc e : 0.5 mm $\varepsilon = \frac{0.5}{\mathrm{M}}$, $M = \frac{a(1 - e^2)}{(1 - e^2 \sin^2(\varphi_0))^3}$,

a : semi - major axis, e : eccentrici ty, $N = \frac{a}{\sqrt{1 - e^2 \sin^2(\varphi)}}$

The second step is to calculate the orthometric height, H, as shown in Equation 8. This calculation needs to know the Mars geoid (areoid) undulation N. In our study, the average undulation value from Mars Orbital Laser Altimeter (MOLA) profiles in a landing site is used for the undulation value for the corresponding study area. .Because one MOLA profile covers the beginning and end part of an image, the average undulation of the MOLA footprints can be a good approximation for the entire stereo model. From MOLA PEDR, orthometric height which is the height between Mars surface and Mars areoid is provided and it was calculated by the laser measurement processing. In addition, spherical latitude, longitude and orthometric height provided in the PEDR files can be converted to ellipsoid latitude, longitude and height. Therefore, the undulation of the MOLA points can be calculated according to Equation 8

$$H = h - N \tag{8}$$

where, H is orthometric height, h is ellipsoid height and N is geoid undulation.

Map Projection

Map projection is a representation of a point with three coordinates, either Cartesian coordinates or geographical coordinates, on surface as a two-dimensional plane. Map projection is necessary to generate DEM before height interpolation. Equidistance cylindrical map projection is used for this study. The radius of a spheroid for map projection is 3,396.190 meters. Table 2 shows central meridian and reference latitude of each site.

Table 2. Central meridian and Reference latitude for map projection

	EOS chasma	Gusev crater	Isidis Planitia
Central meridian	318.638	175.940	84.848
Reference latitude	-13.450	-14.960	4.609

DEM interpolation

When DEM is generated, elevation values need to be interpolated to a regular spacing. Elevation values are calculated using known surrounding points, then those are stored in a grid format with projected equal X and Y spacing. As a digital product, various visualization methods, such as hill shading and relief are used to represent the grid format DEM.

In order to model surface accurately with irregular points collected from surface, various interpolation methods are suggested and investigated (Longley et al. 1999). In this study, Kriging interpolation is applied. Burshtynska and Zayac (2002) reported Kriging method is the optimal method for DEM generation as a statistical method. The ordinary Kriging method determines the elevation value based on distances among surrounding points as well as the weights which are derived from statistical analysis.

$$\hat{z}(x_0) = \sum_{i=1}^{n} \lambda_i \cdot z(x_i)$$

$\hat{z}(x_0)$: interpolated value

n : the number of points considered as surrounding points

λ_i : the weight of the i th surrounding point $\sum_{i=1}^{n} \lambda_i = 1$

$z(x_i)$: value of a surrounding point (9)

Equation 9 represents the ordinary Kriging interpolation method (Burrough and McDonnell, 1998), and explains its implementation. The interpolated value of a point is determined by the number of surrounding points (n), the weights (λ) which are calculated by distances and a chosen statistical model. After the number of surrounding points which affect the determination of an interpolated value of a point is set up, the weight value of each surrounding point is determined by the distance from the interpolated point and the spatial statistics model. The weights of all surrounding points are summed to 1. In this study, spherical model is chosen as a variogram which is a model of the spatial pattern and variation. The regularly interpolated cell size is 10 meters, which is equivalent to about two pixels on the MOC narrow angle image. Following figures are presenting the results of the generated DEM for three candidate landing sites. Figure 8 shows the hillshaded DEM generated by Kriging method.

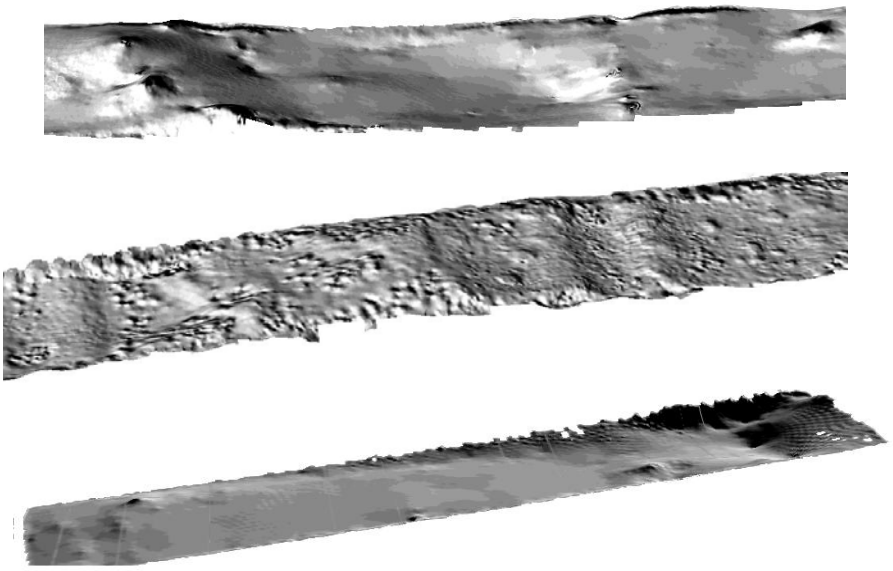

Figure 8. Hillshaded DEM (top: EOS; middle: Gusev; bottom: Isidis)

CONCLUDING REMARKS

Generating high resolution DEM for Mars surface presents difficulties to existing commercial tools. Special treatment is needed to obtain quality products. The presented triangulation based hierarchical matching approach proves to be effective. It consists of a three-step matching scheme: initial prediction via polynomial interpolation, refinement via cross correlation and final precision location by using the least squares matching. This scheme is used recursively by each time adding a point inside a triangle element based on an objective function that considers both its radiometric distinction and its geometric location. Through this approach, sufficiently large number of corresponding points can be generated for DEM production. A cross validation analysis indicates that 90% such matched points are better than 1 pixel. As for DEM generation, Kriging method is shown to be superior to other interpolation approaches. Results from three selected MER candidate landing sites demonstrate the effectiveness of the proposed image matching and DEM interpolation methodology.

REFERENCES

[1] Burrough, P.A. and R.A. McDonnell (1998). Principles of Geographical information systems, Oxford university press, pp.139.

[2] Burshtynska, K and A. Zayac (2002). Application of Differential Splines for Relief Simulation, ISPRS Symposium on Geospatial Theory, Ottawa

[3] Ivanov, A.B., and J.J. Lorre (2002). Analysis of Mars Orbiter camera stereo pairs, The 33rd Lunar and Planetary Science Conference, March 11–15, League City, TX.

[4] Kirk, R.L., L.A. Soderblom, E. Howington-Kraus, and B. Archinal (2002). USGS High resolution topomapping of Mars with Mars Orbiter Camera Narrow-angle Images, IAPRS, Vol.34, Part 4, "Geospatial Theory,Processing and Applications", Ottawa, CD-ROM.

[5] Longley, P.A., M.F. Goodchild, D.J. Maguire and D.W. Rhind (1999). Geographical information systems, John Wiley & Sons, Inc., vol. 1. pp 448-449.

[6] Mikhail, Edward, James S. Bethel, J. Chris McGlone, Introduction to Modern Photogrammetry, 2001, John Wiley & Sons, Inc.